

Using a CCD camera lidar system for detection of Asian dust

Jalal Butt^a, Chris Oville^a, Nimmi C.P. Sharma^a, and John E. Barnes^b

^aDepartment of Physics and Engineering Physics, Central Connecticut State University, New Britain, CT 06053, USA

^bCooperative Institute for Research in Environmental Sciences (CIRES), University of Colorado, Boulder, CO 80309, USA and NOAA Earth System Research Laboratory, Global Monitoring Division (GMD), Boulder, CO 80305, USA

ABSTRACT

During intense spring and early summer storms, substantial volumes of dust from east Asian desert regions are lofted over the continent and transported by prevailing winds across the Pacific Ocean. The phenomenon has wide reaching effects including long range nutrient and sediment transport as well as radiative forcing. Mauna Loa Observatory (MLO) is an atmospheric baseline station in Hawaii at an altitude of 3397-m.a.s.l.. MLO's CCD Camera Lidar (CLidar) has fine near-ground altitude resolution, which makes it a useful system for Asian dust detection, especially at high altitude sites such as MLO. A 20-Watt, 532-nm Nd:YAG laser was vertically transmitted into the atmosphere above MLO. The side-scatter from atmospheric constituents, such as clouds, aerosols, and air molecules was detected by a wide-angle CCD camera situated 139-m from the laser. The obtained signal was range-normalized using a molecular scattering model and corrected for transmission with a column-averaged aerosol phase function derived from MLO-based AERONET photometer measurements. In several of the resulting aerosol extinction profiles, notable aerosol layers were observed near altitude ranges in which Asian dust is typically transported by prevailing winds. Corresponding relative humidity measurements made by nearby radiosondes were examined to differentiate aerosol scattering from cloud scattering. To further examine layers exhibiting both aerosol extinction peaks and relative humidity levels below that of tenuous ice clouds, back trajectories were conducted using NOAA's Hybrid Single Particle Lagrangian Integrated Trajectory model. Several layers from 2008 and 2009 were traced back to East Asian deserts.

Keywords: Asian dust, dust transport, Mauna Loa Observatory, CCD camera lidar, CLidar, East Asian deserts, Asian dust detection, dust detection

1. INTRODUCTION

Asian dust is a meteorological phenomena that occurs in the early-spring to summer months in Eastern Asia. During this period, dust activity intensifies in Northeastern Chinese and Southern Mongolian deserts as a result of high-speed surface winds, which have been found to be associated with the Mongolian cyclonic depression and regional frontal systems.^{1,2} The high-speed surface winds initially loft up the desert dust. Dust is then further elevated by complex turbulent motion, which can reach altitudes high enough to become entrained in westerly winds. These westerly prevailing winds transport substantial amounts of mineral dust across Eastern Asia and across large distances over the Pacific Ocean.^{3,4} Previous studies have shown that mineral dust transport from Eastern Asia to the Pacific Ocean significantly contributes to the mineral dust deposition flux in the Northern Pacific Ocean.^{5,6}

The significance of Asian dust sediment and nutrient deposition in the Pacific Ocean help demonstrate the importance of continuous monitoring of mineral dust transport across the Pacific Ocean. One potential location

Further author information:

Jalal Butt: E-mail: jbutt@my.ccsu.edu

Chris Oville: E-mail: coville@my.ccsu.edu

Nimmi C.P. Sharma: Email: sharmanim@ccsu.edu

to make these observations is Hawaii. Darzi et al state that the National Oceanic and Atmospheric Administration's (NOAA) Mauna Loa Observatory (MLO) on the Big Island of Hawaii (see figure 1) is an excellent location to make observations of Asian dust.⁷



Figure 1: Mauna Loa Observatory and the East Asian Taklamakan and Gobi Deserts. (Google)

Due to its elevation and relative isolation, the atmospheric column above MLO has relatively little anthropogenic aerosol influence. In addition, the island site is in the path of westerly prevailing winds known to transport East Asian air across the Pacific Ocean.

With its suite of world-class atmosphere-probing instruments, MLO is also well equipped for Asian dust Detection. The observatory is home to a stratospheric lidar, a nephelometer, a robotic sun photometer, and a charge-coupled device (CCD) camera lidar (CLidar). Because Asian Dust can be found over a wide range of altitudes – including those close to the ground at high altitude sites such as MLO – the CLidar can be particularly useful since it can measure aerosols all the way down to ground level, without the field of view effects of a monostatic lidar.⁸ This study uses the CLidar to support observations of Asian dust transport over MLO. CLidar measurements are used in conjunction with relative humidity data from local radiosondes and air parcel back-trajectories from an air parcel back-tracing model.

2. METHODOLOGY

2.1 Experimental Setup

The CLidar at MLO utilizes a vertically transmitted, linearly-polarized, 20Watt, 532nm Nd:YAG pulsed laser beam with energies varying from 300mJ to 600mJ, and a pulse width of 8ns. The wide angle optics of the camera-detector, (which, for the data presented in this study, were separated from the optical transmission axis by 139m) permit imaging of the full height of the beam in a single exposure. As a result, unlike conventional lidar in which the altitude of the detected backscatter is time-resolved, the detected sidescatter of the CLidar is *geometrically* resolved. A schematic of the CLidar system is shown in figure 2.

For each CLidar experiment, multiple 332 second exposures are imaged (often over several hours) including a single "dark frame" – an exposure taken with the camera's lens covered. The time-integrated signal for each exposure (an image file) is then processed, and aerosol extinction is calculated.

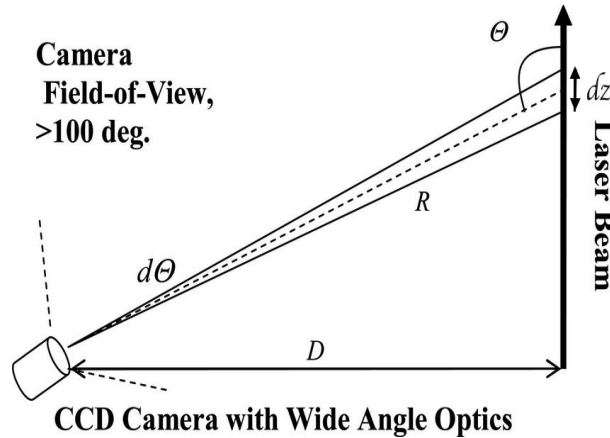


Figure 2: CLidar Schematic: Each pixel in the CCD array detects a constant angle $d\theta$ which corresponds to beam length, dz . With D held constant, dz is dependent on altitude. The altitude resolution for the setup is good to several km above ground level.

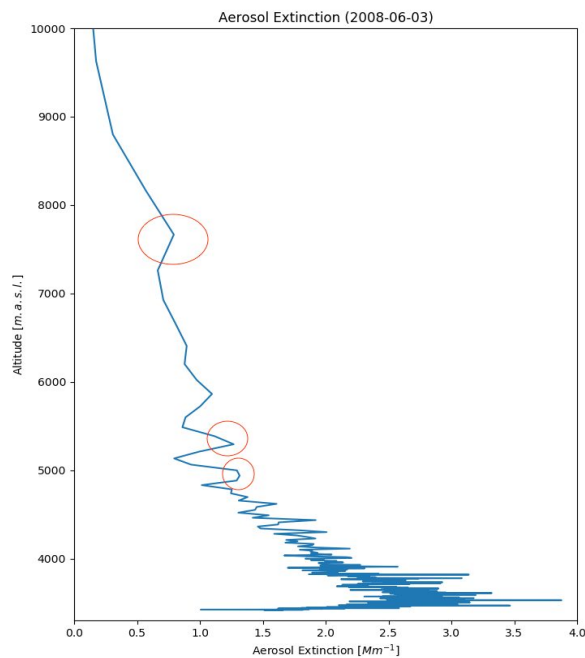
2.2 Image Processing

The goal of image processing is to convert side-scatter to extinction, which is achieved by correcting for instrumentation biases, subtracting background light, normalizing for molecular scattering, and correcting for transmission. First, since an operating CCD produces idiosyncratic "dark current" which would otherwise be recorded as light intensity, any signal present (including "hot pixel" signal) in the dark frame (section 2.1) is subtracted from each normal exposure file. Then background light (including light from stars) is subtracted using a gaussian plus constant fitting function for each beam cross-section. Next, pixel intensities, which are due to a combination of scattering from both air molecules and particulates are corrected to derive particulate-only scattering by applying a molecular scattering model which is normalized to an aerosol-free atmospheric layer. Because the remaining measured intensity is influenced by the angle-dependent scattering efficiency of the aerosols in the path of the laser, a phase function derived from NASA's Aerosol Robotic Network (AERONET) is needed. The signal profile is then corrected for both molecular and aerosol transmission. Usually two or three iterations are enough for the transmission correction to converge using the phase function, with the additional assumption of a single scattering albedo. MLO is host to one of AERONET's array of sun photometers, so the phase functions used are spatially consistent with each CLidar dataset; however, the photometer measurements are taken several hours before the evening CLidar runs and are column-averaged.

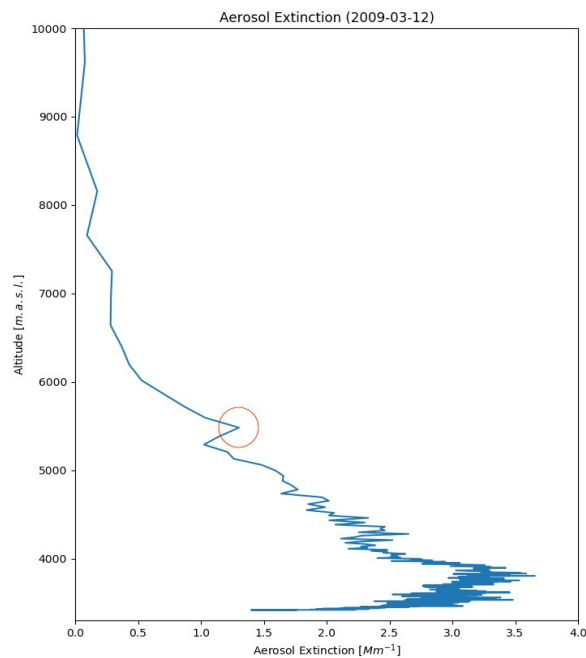
3. DATA ANALYSIS

The CLidar system has been operated at Mauna Loa Observatory for multiple years beginning in 2006.⁹⁻¹¹ In this investigation, CLidar data taken at MLO during spring and summer months is examined, as the intensified dust activity in Eastern Asia that largely contributes to the trans-Asia and trans-Pacific dust occurs during these months. After correcting the raw lidar signals and computing the aerosol extinction profiles, the profiles were time-averaged over each night's CLidar operation. Several of these average profiles had aerosol features in the altitude range where Asian dust is expected to be entrained in westerly prevailing currents. Data examined from two nights of experimental operations exhibited notable aerosol extinction layers represented by local maxima, as shown in figure 3.

Figure 3a shows 2008-06-03 UTC's calculated aerosol extinction profile with three highlighted extinction features of interest: the first near 4900 meters above sea level (masl), second near 5200masl, and third near 7600masl. Figure 3b shows 2009-03-12 UTC's calculated aerosol extinction profile with one highlighted extinction feature of interest near 5400masl. Aerosol extinction provides some information on the scattering properties of the scatterer but is not sufficient information to make conclusions on the type of scatterer (ice crystals, dust, etc.), so the features can plausibly be one of many aerosols. Asian dust features in these aerosol extinction profiles can especially resemble tenuous ice-clouds. Hence, it is of particular importance to ensure that the aerosol



(a) Altitude vs. Aerosol Extinction for 2008-06-03 UTC with highlighted aerosol layers of interest.



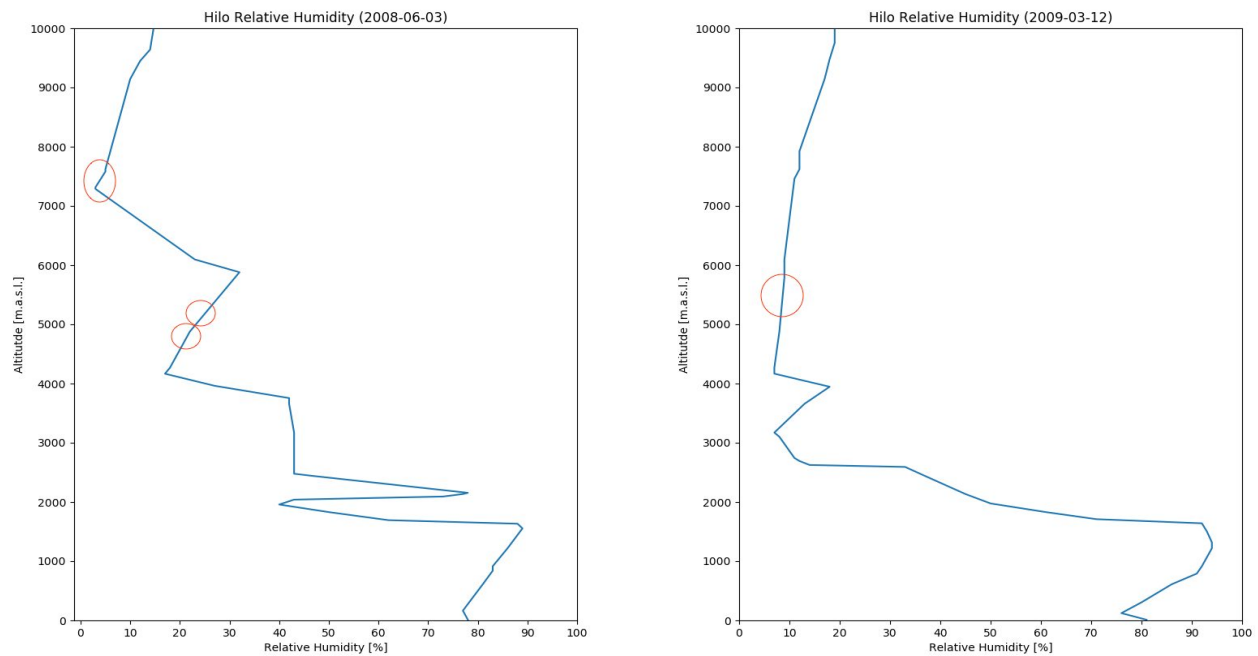
(b) Altitude vs. Aerosol Extinction for 2009-03-12 UTC with highlighted aerosol layer of interest.

Figure 3: Aerosol extinction profiles for dates with notable aerosol extinction features.

extinction feature is not a measurement of a cloud. The local Hilo radiosonde station deploys radiosondes every 12 hours and is located approximately 60km from MLO. Hilo radiosondes collect a range of data, including atmospheric pressure, temperature, wind speed and direction, and relative humidity, all as functions of altitude. Radiosonde data can be useful to support observations of Asian dust because its relative humidity measurements can suggest whether or not an aerosol feature in a particular altitude range exhibits relative humidity levels that of a cloud.^{12,13} Note that relative humidity levels for ice clouds is tightly distributed around 100%, with levels below 70% indicating cloud-free altitudes.^{12,14} One of the twice-daily radiosonde deployments are taken within several hours of CLidar operation, so its relative humidity measurements can be used to differentiate ice clouds from other aerosols. Relative humidity profiles corresponding to the aerosol extinction profiles in figure 3 are shown in figure 4.

Figure 4a shows the relative humidity profile from 2008-06-03 UTC with the altitudes of the aerosol extinction features of interest from this date highlighted (4900masl, 5200masl, and 7600masl). Figure 4b shows the relative humidity profile from 2009-03-12 UTC with the altitude of the aerosol extinction feature of interest from this date also highlighted. The altitude ranges in which the three aerosol layers of interest are observed on 2008-06-03 UTC all have relative humidity levels measured to be lower than 70% (RH(4900masl) = 22%; RH(5200masl) = 25%; RH(7600masl) = 5%). The altitude range in which the aerosol layer of interest is observed on 2009-03-12 UTC also has relative humidity levels measured to be lower than 70% (RH(5400masl) = 9%). These relative humidity measurements suggest that the aerosol layers are not tenuous ice clouds, an important conclusion for Asian dust observations from MLO.

Aerosol extinction data show notable features characteristic of aerosol layers, and relative humidity measurements suggest that these layers are not tenuous ice clouds – an important conclusion for Asian dust observations from MLO. These features had their geographic origins traced using NOAA's HYbrid Single Particle Lagrangian Integrated Trajectory (HYSPLIT) model. The HYSPLIT model is a hybrid of the Eulerian fixed reference frame



(a) Hilo relative humidity profile measured at 12:00 2008-06-03 UTC.

(b) Hilo relative humidity profile measured at 12:00 2009-03-12 UTC.

Figure 4: Relative humidity measurements taken by radiosondes launched from Hilo, HI with altitudes corresponding to aerosol layers of interest highlighted.

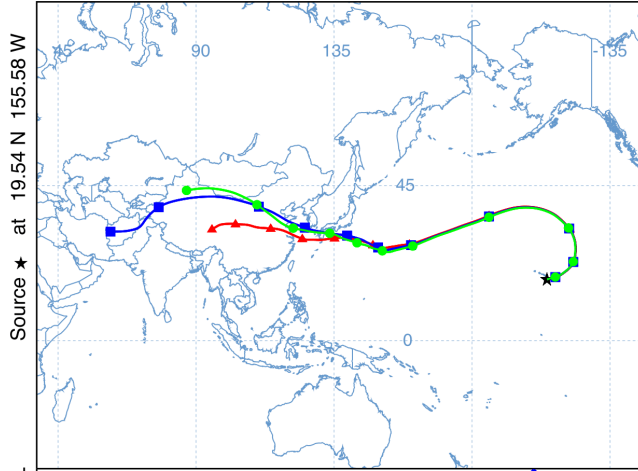
method and the Lagrangian moving reference frame method. The Eulerian method is used to calculate pollutant air concentrations; and the Lagrangian method is used to calculate air-mass diffusion and advection as the particles move in space.¹⁵

4. RESULTS

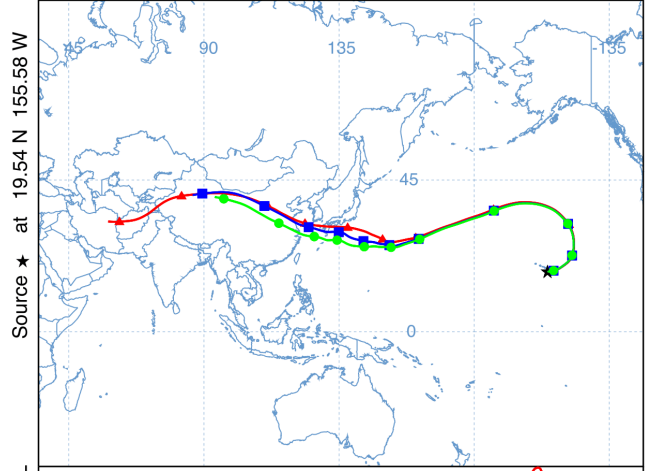
Back-trajectories of air-parcels at the spatio-temporal coordinates of the observed aerosol features were conducted, the results of which are shown in figure 5.

Figure 5a-5d are each figures with three back-trajectories at unique altitudes of air-parcels in the respective aerosol feature altitude range. These figures show three back trajectories at three different altitudes within the respective aerosol layer to show the consistency of the layers' geographic origins. Figure 5a shows that the air parcels (triangles [tri]: 4900masl, squares [sq]: 4950masl, circles [cir]: 5000masl) in 2008-06-03 UTC's 4900masl feature altitude range consisted of aerosols entrained in air that passed through the arid Gobi and Taklamakan Deserts and took 10-11 days to transport to MLO. Figure 5b shows that the air parcels (tri: 5210masl, sq: 5295masl, cir: 5325masl) in 2008-06-03 UTC's 5200masl feature range consisted of aerosols that were also entrained in air that passed through the Gobi and Taklamakan Deserts and took 10-11 days to transport to MLO. Similar results were obtained for 2008-06-03 UTC's 7600masl feature, where the air parcels (tri: 7500masl, sq: 7650masl, cir: 7700masl) in the feature altitude region were entrained in westerly currents that transported the aerosols over the Taklamakan Desert to MLO in 9-10 days. Figure 5d shows that the air parcels (tri: 5360masl, sq: 5380masl, cir: 5400masl) in 2009-03-12 UTC's 5400masl feature range contained aerosols entrained in air currents that transported the aerosols through the northern Gobi Desert to MLO in 7-8 days.

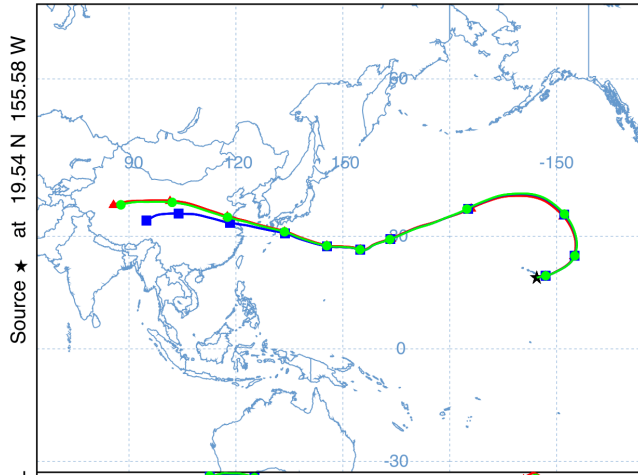
The aerosol extinction features were recognized for their potential to be Asian dust in-part due to their characterization as local maxima. Then, it would be reasonable to suspect that adjacent local minima may represent



(a) HYSPLIT back-trajectory of air-parcels in the 4900masl region on 2008-06-03 UTC.



(b) HYSPLIT back-trajectory of air-parcels in the 5200masl region on 2008-06-03 UTC.



(c) HYSPLIT back-trajectory of air-parcels in the 7600masl region on 2008-06-03 UTC.



(d) HYSPLIT back-trajectory of air-parcels in the 5400masl region on 2009-03-12 UTC.

Figure 5: HYSPLIT back-trajectories for the aerosol features observed on 2008-06-03 UTC and 2009-03-12 UTC originating from the respective altitude at MLO during the time of CLidar operation. ★ represents MLO's geographic location; each colored back-trajectory represents a unique altitude used; each colored shape (unique to each back-trajectory) represents a successive span of 24 hours back-stepped from the time of observation.

cleaner parcels of air - air that doesn't consist of Asian dust, with the cleanest of these originating from the Pacific Ocean. Back-trajectories of *clean* air parcels are shown in figure 6. Figure 6 shows that the back-trajectories of air parcels at local minima relative to the aerosol features trace back to the coasts of Japan and the Philippines; and the Pacific Ocean.

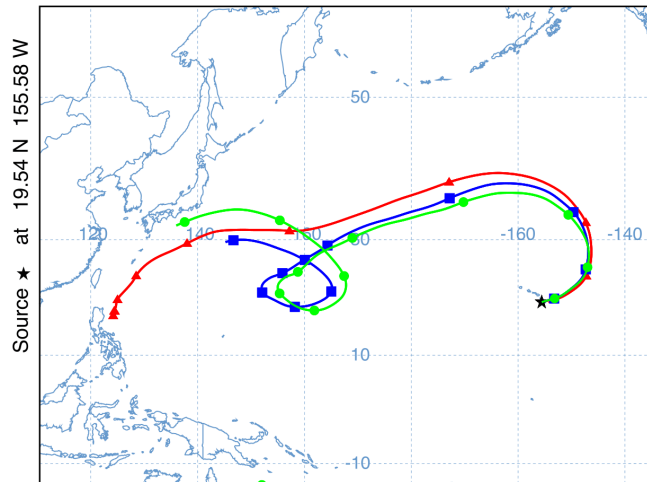


Figure 6: HYSPLIT 10.5-day back-trajectory of 2008-06-03 UTC air parcels from altitude ranges in which aerosol extinction is a local minimum (tri: 4830masl, sq: 5485masl, cir: 6200masl).

5. DISCUSSION

This investigation's objective was to track Asian dust transport from Eastern Asia in westerly air currents as it crossed over Mauna Loa Observatory. These back-trajectory results show that most of the tropospheric aerosol column above MLO is generally quite clean. However, the aerosol extinction (figure 3), humidity levels (figure 4), and geographic origins (figure 5) of particular aerosol layers observed in CLidar measurements at MLO suggest that these layers are dry aerosols originating from arid East Asian deserts during Asian dust season. The large amount of Asian dust observed to be transported across the Pacific Ocean has a significant impact on remote nutrient and sediment deposition, the earth's radiative balance, and other mass transport. The observations of Asian dust on 2008-06-03 UTC are interesting in that there were multiple dust observations at unique altitudes, and that all of the observed dust layers on this night were traced back to the same region. This calls for further study on the westerly wind-currents and the effect their short and long term variability may have on the efficiency of trans-Pacific mineral dust transport. The CLidar system is capable of making observations of Asian dust transport at MLO, in conjunction with relative humidity measurements and air parcel back-trajectory modeling.^{16,17} Continuous monitoring of Asian dust over the Pacific Ocean is imperative for longitudinal studies of the dust transport, which could also potentially support studies of sediment and mineral deposition in the Pacific Ocean; and studies of the impact of Asian dust transport on regional radiative forcing.

ACKNOWLEDGMENTS

This project is based upon work supported by the National Science Foundation under grant #0311143. Any opinions, findings, and conclusions or recommendations expressed in this material are those of the author(s) and do not necessarily reflect the views of the National Science Foundation.

The authors acknowledge AERONET and Brent Holben of NASA Goddard Space Flight Center for their efforts in establishing and maintaining the Mauna Loa AERONET site.

The presentation of this paper was supported by the John and Jane Mather Foundation.

Map data ©2018 Google.

REFERENCES

1. K. Kawai, K. Kai, Y. Jin, N. Sugimoto, and D. Batdorj, "Dust event in the gobi desert on 22-23 may 2013: Transport of dust from the atmospheric boundary layer to the free troposphere by a cold front," *SOLA* **11**, pp. 156–159, 2015.
2. J. Sun, M. Zhang, and T. Liu, "Spatial and temporal characteristics of dust storms in china and its surrounding regions, 1960–1999: Relations to source area and climate," *Journal of Geophysical Research: Atmospheres* **106**(D10), pp. 10325–10333, 2001.
3. Y. Iwasaka, M. Yamato, R. Imasu, and A. Ono, "Transport of asian dust (kosa) particles; importance of weak kosa events on the geochemical cycle of soil particles," *Tellus B* **40**(5), pp. 494–503, 1988.
4. F. H. Tu, D. C. Thornton, A. R. Bandy, G. R. Carmichael, Y. Tang, K. L. Thornhill, G. W. Sachse, and D. R. Blake, "Long-range transport of sulfur dioxide in the central pacific," *Journal of Geophysical Research: Atmospheres* **109**(D15), 2004.
5. R. Duce, C. Unni, B. Ray, J. Prospero, and J. Merrill, "Long-range atmospheric transport of soil dust from asia to the tropical north pacific: Temporal variability," *Science* **209**(4464), pp. 1522–1524, 1980.
6. Y. Iwasaka, H. Minoura, and K. Nagaya, "The transport and spacial scale of asian dust-storm clouds: a case study of the dust-storm event of april 1979," *Tellus B: Chemical and Physical Meteorology* **35**(3), pp. 189–196, 1983.
7. M. Darzi and J. W. Winchester, "Aerosol characteristics at mauna loa observatory, hawaii, after east asian dust storm episodes," *Journal of Geophysical Research: Oceans* **87**(C2), pp. 1251–1258.
8. J. Harms, "Lidar return signals for coaxial and noncoaxial systems with central obstruction," *Appl. Opt.* **18**, pp. 1559–1566, May 1979.
9. J. E. Barnes, N. C. P. Sharma, and T. B. Kaplan, "Atmospheric aerosol profiling with a bistatic imaging lidar system," *Appl. Opt.* **46**, pp. 2922–2929, May 2007.
10. J. E. Barnes, S. Bronner, R. Beck, and N. Parikh, "Boundary layer scattering measurements with a charge-coupled device camera lidar," *Applied Optics* **42**(15), pp. 2647–2652, 2003.
11. N. C. Sharma and J. E. Barnes, "Wide-angle imaging lidar for high-resolution near-ground aerosol studies," in *Optical Sensors*, pp. JT3A–23, Optical Society of America, 2013.
12. J. Ovarlez, J.-F. Gayet, K. Gierens, J. Ström, H. Ovarlez, F. Auriol, R. Busen, and U. Schumann, "Water vapour measurements inside cirrus clouds in northern and southern hemispheres during inca," *Geophysical Research Letters* **29**(16), pp. 60–1–60–4.
13. J. Ström, M. Seifert, B. Kärcher, J. Ovarlez, A. Minikin, J.-F. Gayet, R. Krejci, A. Petzold, F. Auriol, W. Haag, R. Busen, U. Schumann, and H. C. Hansson, "Cirrus cloud occurrence as function of ambient relative humidity: a comparison of observations obtained during the inca experiment," *Atmospheric Chemistry and Physics* **3**(5), pp. 1807–1816, 2003.
14. A. J. Heymsfield and L. M. Miloshevich, "Relative humidity and temperature influences on cirrus formation and evolution: Observations from wave clouds and fire ii," *Journal of the atmospheric sciences* **52**(23), pp. 4302–4326, 1995.
15. A. Stein, R. R. Draxler, G. D. Rolph, B. J. Stunder, M. Cohen, and F. Ngan, "Noaa's hysplit atmospheric transport and dispersion modeling system," *Bulletin of the American Meteorological Society* **96**(12), pp. 2059–2077, 2015.
16. N. C. Sharma and J. E. Barnes, "Identifying asian dust with digital imaging of atmospheric laser light scatter," in *Geoscience and Remote Sensing Symposium (IGARSS), 2016 IEEE International*, pp. 5585–5588, IEEE, 2016.
17. J. Butt, N. C. Sharma, and J. E. Barnes, "Lidar observations of long range dust transport over mauna loa observatory," in *Lidar Remote Sensing for Environmental Monitoring 2017*, **10406**, p. 104060M, International Society for Optics and Photonics, 2017.